Suppression of broadband noise at mode locking in driven vortex matter

S. Okuma and J. Inoue
Research Center for Low Temperature Physics, Tokyo Institute of Technology, 2-12-1, Ohokayama, Meguro-ku, Tokyo 152-8551, Japan

N. Kokubo
Center for Research and Advancement in Higher Education, Kyushu University, 4-2-1, Ropponmatsu, Chuoh-ku, Fukuoka 810-0044, Japan

(Received 19 September 2007; published 15 November 2007)

We measure voltage noise generated by current-driven vortices for fields corresponding to the solid phase when at equilibrium including the peak-effect regime, focusing on a change in broadband noise (BBN) as the vortex system undergoes a mode-locking (ML) resonance. For all the fields steplike structure indicative of ML is observed in the *I-V* curves. We find that BBN at high frequencies (but well below the ac drive frequency) is suppressed inside the ML steps. The results are consistent with the view that the mode-locked state is a frozen solid pinned in the moving frame of reference.

DOI: 10.1103/PhysRevB.76.172503 PACS number(s): 74.40.+k, 62.20.Fe, 74.25.Qt, 74.78.Db

When an object moves in a periodic potential in the presence of combined dc and ac forces, steplike structure analogous to Shapiro steps found in Josephson junctions appears in the force-velocity (F-v) characteristics. This phenomenon called a mode-locking (ML) resonance has been observed in several physical systems with many degrees of freedom, which include the charge density waves,[1,2] spin density waves,[3] and driven vortices in type-II superconductors.[4–10] The steps in the F-v curves appear, when the internal frequency f_{int} of the system locks to the external frequency f_{ext} of the ac drive, more precisely, when the relation $qf_{int} = pf_{ext}$ is satisfied, where p and q are the integers. The ML resonance for driven vortices has been observed not only in superconductors with periodic pinning[6,7] but also in those with *random* pinning,[4,8,9] such as amorphous films studied in this paper, where a periodicity can be induced dynamically as a result of the coherent motion[11–13] of a vortex lattice.

It is well known that, in the presence of random pinning, several dynamic phases of driven vortices with different temporal, positional, and orientational orders are realized depending on the amplitude of F and v. Some of them, including plastic and smectic flows,[14] accompany large broadband noise (BBN) due to pinning induced incoherent flow of vortices, as seen in numerical simulations.[15,16] In experiments, BBN has been clearly observed not only near the critical current I_c but also in a moderate dc current range well above I_c, where the influence of random pinning is effectively reduced and elasticity is locally recovered by driving force. Thus, an interesting question arises as to how BBN changes, when the moving vortex matter is mode locked. It has been shown earlier for the CDW condensate[1] that ML yields a decrease in the narrowband noise width, which scales with the BBN amplitude. For a driven vortex system, it has been predicted numerically that BBN should be suppressed at ML,[17] while no experimental verification has been reported so far. It is also known that largest BBN due to driven vortices appears in the peak-effect (PE) regime.[18–20] This is because pinning for vortices is enhanced by softening of the vortex lattice just prior to melting or disorder-induced destruction of long-range order.[21] Here we perform the measurements of BBN generated by the current-driven vortices for fields corresponding to the solid phase when at equilibrium including the PE regime of a thick amorphous (a-)Mo_xGe_{1-x} film, focusing on a change in BBN as the system undergoes ML.

For all the fields steplike structures (ΔI) indicative of ML are observed in the dc current-voltage (I-V) curves in the presence of superimposed ac drive. The spectral shape at low frequencies f is of Lorentzian type, while at high f (but well below the ac drive frequency f_{ext}) it is almost white. By changing I, BBN at high f shows clear suppression or disappearance inside the ML steps, although the suppression as well as ML is degraded just prior to (dynamic) melting. The results are consistent with the view that the mode-locked state is a frozen solid pinned in the moving frame of reference.[17] The preliminary data related to present work have been reported elsewhere.[22]

We prepared the 330-nm-thick a-Mo_xGe_{1-x} film by rf sputtering on a Si substrate held at room temperature.[10] The mean-field transition temperature T_{c0} defined by a 95% criterion,[23] i.e, the linear resistivity ρ decreases to 95% of the normal-state resistivity, is 5.86 K and the zero-resistivity temperature T_c is 5.78 K. We measured ρ, I-V characteristics, and the voltage noise spectrum $S_V(f)$ induced by the currents using a four-terminal method. The ac (rf) current I_{rf} was applied through an rf transformer. The frequency f_{ext} and amplitude of I_{rf} are 10 MHz and 0.07–0.50 mA, respectively. In measuring $S_V(f)$ over a broad frequency range $f = 1$ Hz–40 kHz, the voltage enhanced with a preamplifier was analyzed with a fast-Fourier transform spectrum analyzer.[23] We obtained the excess noise spectra $S_V(f)$ by subtracting the background contribution, which was measured with $I = I_{rf} = 0$.[24] The sample was directly immersed into liquid ^{4}He. The field B was applied perpendicular to the plane of the film.

In Fig. 1(a) we plot the (dc) critical current I_c (open circles) at 4.0 K against B, where I_c is defined as a threshold current at which the vortices start to move. The values of I_c for different B are extracted from the I-V curves using a 10^{-7} V criterion. We also plot a "dynamic" critical current

 ©2007 The American Physical Society

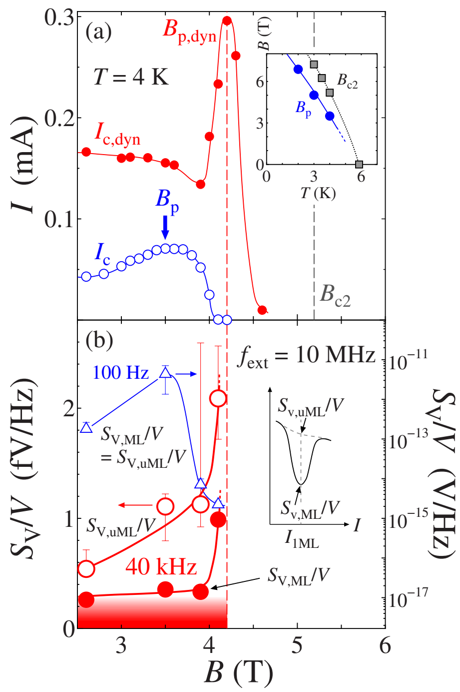

FIG. 1. (Color online) (a) Critical current I_c (open circles) and dynamic critical current $I_{c,dyn}$ (full circles) at 4.0 K against B. Vertical dashed lines represent the location of $B_{p,dym}$ (left) and B_{c2} (right). Inset: B_{c2} (squares) and B_p (circles) against T. (b) B dependences of $S_{V,ML}/V$ (full circles) and $S_{V,uML}/V$ (open circles) for 40 kHz at 4.0 K. Open triangles correspond to $S_{V,ML}/V(=S_{V,uML}/V)$ for 100 Hz. A shaded zone represents the background level. Inset: Schematic illustration of determination of $S_{V,ML}/V$ and $S_{V,uML}/V$ at I_{1ML} (a vertical dashed line). Other lines are guides for the eye.

$I_{c,dyn}$, which is determined by linear extrapolation of the flux-flow (linear) part of I-V curves to the zero voltage. It has been shown recently that $I_{c,dyn}$ reflects the pinning strength for driven vortices in the flux-flow state.[10] One can see a broad peak of $I_c(B)$ in the field region B=2.6–4.1 T (the peak field B_p is ≈3.5 T) and a more pronounced peak of $I_{c,dyn}(B)$ in B=3.9–4.6 T. The peak field $B_{p,dyn}$(=4.2 T) of $I_{c,dyn}$ is higher than that of B_p of $I_c(B)$ and very close to a field ~4.1 T where I_c vanishes, consistent with recent results.[10] All of the data were taken at 4.0 K in B=2.6 T (the onset of the peak in I_c), 3.5 T (≈B_p), 3.9 T (the onset of the peak in $I_{c,dyn}$), and 4.1 T (just prior to $B_{p,dyn}$). In the inset of Fig. 1(a) we plot the upper-critical field B_{c2} defined by a 95% criterion [23] and B_p against T.

Shown in Fig. 2(a) are the $I(V)$ curves measured with superimposed (10 MHz) rf currents of different amplitudes (I_{rf}=0.135–0.252 mA) at 4.0 K in 3.5 T (≈B_p). The steplike behavior suggestive of ML is observed at the two voltage levels V_p; V_1=0.58±0.04 mV and V_2=1.13±0.04 mV. The location as well as the existence of the steps can be more clearly seen by plotting the differential conductance dI/dV against V, as shown in Fig. 2(b). Assuming a triangular vortex array moving in the direction parallel to one side of the triangle(s), i.e., the lattice period a in the direction of vortex motion is equal to the nearest-neighbor distance of the triangular vortex array, $(2\Phi_0/\sqrt{3}B)^{1/2}$, as schematically illustrated in the inset of Fig. 2(a), a fundamental voltage step (p=q=1) is calculated to be $V_{1/1}$=0.57±0.02 mV from the equation $V_{p/q}=lvB=l(p/q)f_{ext}aB$, where Φ_0 is the flux quantum and l is the distance between the voltage probes. The value of $V_{1/1}$=0.57 mV thus calculated well coincides with the observed V_1=0.58±0.04 mV, $V_2/2$=0.57±0.02 mV, and $V_3/3$=0.57±0.01 mV (not shown here). These results indicate that the steplike structures in the $I(V)$ curves indeed correspond to ML of the driven vortex lattice. For I_{rf}=0, such steps are no longer visible. The similar smooth steps indicative of ML are observed in other three fields studied (e.g., up to the fifth steps in 2.6 T). We note, however, that not only in this work but also in previous work studying different superconductors[4–10] one cannot observe a sharp step structure with dV/dI=0, such as reported in the CDW condensate. This probably reflects the fact that in the CDW system the sliding motion is nearly one dimensional (1D), while in superconductors the vortex motion is more 2D like, having the transverse degree of freedoms, which makes ML incomplete.

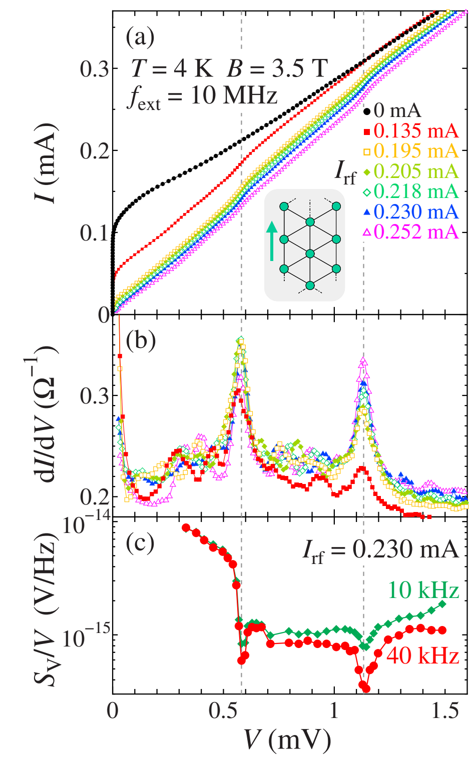

FIG. 2. (Color online) (a) $I(V)$ curves and (b) dI/dV vs V at 4 K in 3.5 T measured with superimposed (10 MHz) I_{rf}, which is listed in (a). Vertical dashed lines represent the location of the first (left) and second (right) ML steps. The inset of (a) illustrates a schematic diagram of triangular vortex arrays, where an arrow indicates the direction of the vortex motion. (c) V dependence of S_V/V at 10 kHz (diamonds) and 40 kHz (circles) measured with superimposed (10 MHz) I_{rf}=0.230 mA at 4 K in 3.5 T. Other lines are guides for the eye.

In the insets of Fig. 3 we display typical noise spectra $S_V(f)/V$ (S_V divided by V) at 4.0 K in 3.5 T in the presence of dc current, I=0.170 mA (top) and 0.350 mA (bottom), but

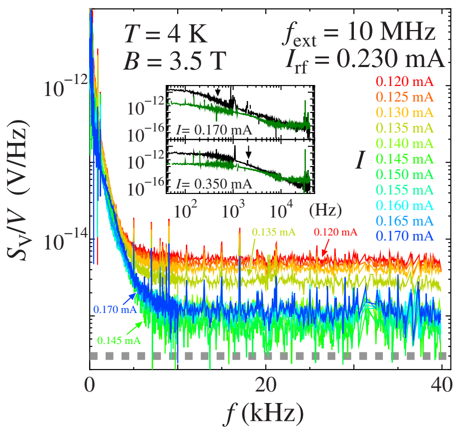

FIG. 3. (Color online) Noise spectra $S_V(f)/V$ at 4 K in 3.5 T in the presence of (10 MHz) I_{rf}=0.230 mA and I (listed in the figure) that covers the first step region. A horizontal dotted line indicates the background level. Insets: $S_V(f)/V$ with I=0.170 (top) and 0.350 mA (bottom) in the absence (black lines) and presence [green (dark gray) lines] of I_{rf}=0.230 mA. Arrows indicate $f_c(=v/w)$.

in the absence of I_{rf} (black lines). Overall spectral shape is of Lorentzian like with a corner frequency, which nearly coincides with a time-of-flight frequency (indicated with an arrow) calculated from $f_c=v/w$, where w is the sample width. Also shown with green (dark gray) lines are $S_V(f)/V$ in the presence of (10 MHz) I_{rf}=0.230 mA superimposed on I. When I_{rf} is superimposed, $S_V(f)/V$ at low $f(<2$ kHz)shows a trend to decrease, while that at high $f(>10$ kHz) shows an increase and takes almost a f-independent value. The decrease of noise at low f with the application of I_{rf} is qualitatively explained in terms of reduced pinning effects by the ac drive, while it remains unclear what causes unusual f-independent noise at high f. Further measurements up to much higher $f(\gg 10^4$ Hz) may be needed to clarify the origin. Independent of this fact, we note that $S_V(f)/V$ at high f contains important information on the vortex dynamics associated with ML, as described below.

In the main panel of Fig. 3 we depict $S_V(f)/V$ at 4.0 K in 3.5 T in the presence of I_{rf}=0.230 mA and dc I that covers the first step region (ΔI_1=0.120–0.170 mA, V_1 =0.58±0.04 mV).[22] With increasing I from 0.120 to 0.145 mA($\equiv I_{1ML}$), $S_V(f)/V$ at *high* $f(>10$ kHz) decreases down to $\approx 6\times 10^{-16}$ V/Hz, which is close to the background level ($\sim 10^{-16}$ V/Hz). With further increasing I, $S_V(f)/V$ then increases. At low $f(<1$ kHz), on the other hand, we do not find any clear change in $S_V(f)/V$ associated with ML (at $I \approx I_{1ML}$) within experimental uncertainty. The results suggest that BBN at high f probes sensitively the change in vortex dynamics associated with ML. In order to see the change in more detail over the broad V including the second step, we plot $S_V(f)/V$ at f=10 kHz (diamonds) and 40 kHz (circles) against V in Fig. 2(c). One can clearly see suppression of S_V/V both at the first and second ML steps.

We now examine how ML and magnitude of noise observed around B_p change in lower and higher fields. In Figs. 4(a)–4(d) we plot V (top), dV/dI (middle), and S_V/V at 40 kHz (bottom) against I, which covers the first step region,

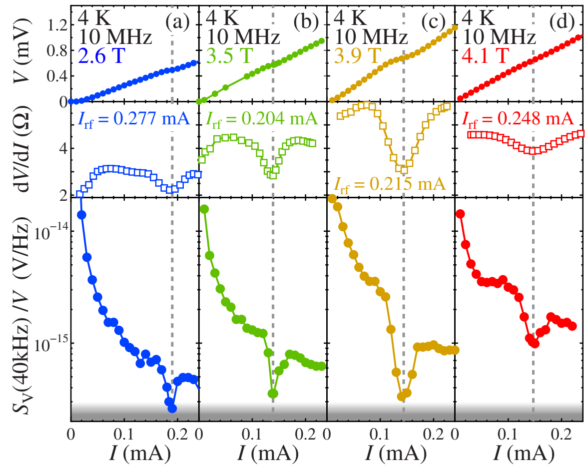

FIG. 4. (Color online) (a) I dependences of V (top), dV/dI (middle), and $S_V(f)/V$ for f=40 kHz (bottom) at 4 K in the presence of superimposed (10 MHz) (a) I_{rf}=0.277 mA in B=2.6 T, (b) 0.204 mA in 3.5 T, (c) 0.215 mA in 3.9 T, and (d) 0.248 mA in 4.1 T. A vertical dotted line in each figure represents the location of I_{1ML} in the first ML step. The background level is indicated by shading.

in the presence of superimposed (10 MHz) I_{rf} in B=2.6, 3.5, 3.9, and 4.1 T, respectively. Here, we focus only on the first ML step and in each B we select I_{rf} yielding a maximum step width ΔI_1. Suppression of BBN [S_V(40 kHz)/V] at ML is clearly visible for all fields. For 2.6, 3.5, and 3.9 T the minimum (base) values of $S_V/V(\equiv S_{V,ML}/V\approx 3\times 10^{-16}$ V/Hz) at an intermediate current ($\equiv I_{1ML}$) in each ML step are close to each other, which are again near the background level shown with a shaded zone. By contrast, $S_{V,ML}/V(\approx 1\times 10^{-15}$ V/Hz) for 4.1 T is remarkably larger. We also notice that in the I region outside the ML step S_V(40 kHz)/V shows a trend to increase with increasing B.

Let us discuss comparatively the field dependences of $S_{V,ML}/V$ (mode-locked state) and $S_{V,uML}/V$ (mode-unlocked state) taken at the same I_{1ML}. Here, $S_{V,uML}/V$ is extracted from the smooth interpolation of the data of $S_V(I)/V$ outside the ML step shown in Fig. 4 (bottom panels) to $I\to I_{1ML}$, as schematically illustrated in the inset of Fig. 1(b). The different values of $S_V(I)/V$ at both ends of the current step ΔI_1 are indicated with error bars. It is seen from Fig. 1(b) that $S_{V,uML}/V$ (open circles) increases with B and grows rapidly, as the peak field $B_{p,dyn}$ for the dynamic $I_{c,dyn}$ is approached, which is similar to the behavior of $I_{c,dyn}(B)$ near $B_{p,dyn}$ in Fig. 1(a). As demonstrated experimentally, the peak in $I_{c,dyn}$ occurs close to the thermally induced, dynamic melting transition of driven vortex lattice.[10] Thus, these results suggest that BBN at high $f(=40$ kHz) may probe increased thermal-shaking effects for vortices just prior to dynamic melting. On the other hand, at low $f(<1$ kHz) the field dependence of BBN is markedly different. The typical data of $S_{V,ML}/V(=S_{V,uML}/V)$ at 100 Hz is plotted in Fig. 1(b) with open triangles, which shows the similarity to $I_c(B)$ rather than to $I_{c,dyn}(B)$. This is consistent with previously reported work in which the generation of low-f BBN near B_p has been observed in various dc-current-driven vortex systems.[20,21]

The most striking finding in this paper is that, except $B \approx B_{p,dyn}$, once the driven vortex system is mode locked, BBN at high f decreases sensitively down to the base values near the background level (indicated by shade), as shown with full circles in Fig. 1(b). In the vicinity of $B_{p,dyn}$, where the ML step in the *I*-*V* curves is degraded and $S_{V,uML}/V$ takes relatively large values, $S_{V,ML}/V$ does not fall down to the background level. According to the simulation by Kolton, Dominguez, and Grønbech-Jensen,[17] inside the ML step (mode-locked state) the vortices are localized, oscillating around their "equilibrium" position seen from a frame of reference moving with velocity determined by V_p at the step position. Thus, the mode-locked state is a *frozen* solid pinned in the moving frame, where only small noise should be generated. Just above (or below) the "depinning" from the ML step some vortices are delocalized, producing coexistence of mode-locked and mode-unlocked channels of flow within the sample. This could be interpreted as a 1D "plastic" depinning or shear slip from the mode-locked state, where relatively large BBN should be generated. Suppression or disappearance of high-f BBN at ML observed over the broad fields corresponding to the solid phase when at equilibrium (in the absence of drive) is consistent with the view of the frozen solid at ML (or ML freezing), although ML does not look complete due probably to the 2D nature of vortex motion, e.g., switching motion of vortices between neighboring flow channels. Degradation of ML and insufficient suppression of BBN at ML observed in the vicinity of $B_{p,dyn}$ are attributed to an increased number of mode-unlocked channels in the sample just prior to (dynamic) melting.

To summarize, we report on BBN generated by driven vortices in the presence of dc and ac currents. We observe steplike structure indicative of ML in the *I*-*V* curves and suppression of high-f BBN inside the steps. Just prior to dynamic melting this feature is less pronounced associated with degradation of ML. The results are consistent with the view that the mode-locked state is a frozen solid pinned in the moving frame of reference.

[1] S. Bhattacharya, J. P. Stokes, M. J. Higgins, and R. A. Klemm, Phys. Rev. Lett. **59**, 1849 (1987); M. J. Higgins, A. A. Middleton, and S. Bhattacharya, *ibid.* **70**, 3784 (1993).

[2] S. N. Coppersmith and P. B. Littlewood, Phys. Rev. Lett. **57**, 1927 (1986) A. A. Middleton, O. Biham, P. B. Littlewood, and P. Sibani, *ibid.* **68**, 1586 (1992).

[3] E. Barthel, G. Kriza, G. Quirion, P. Wzietek, D. Jerome, J. B. Christensen, M. Jorgensen, and K. Bechgaard, Phys. Rev. Lett. **71**, 2825 (1993).

[4] A. T. Fiory, Phys. Rev. Lett. **27**, 501 (1971).

[5] P. Martinoli, Phys. Rev. B **17**, 1175 (1978).

[6] L. Van Look, E. Rosseel, M. J. Van Bael, K. Temst, V. V. Moshchalkov, and Y. Bruynseraede, Phys. Rev. B **60**, R6998 (1999).

[7] C. Reichhardt, R. T. Scalettar, G. T. Zimányi, and N. Grønbech-Jensen, Phys. Rev. B **61**, R11914 (2000).

[8] N. Kokubo, R. Besseling, V. M. Vinokur, and P. H. Kes, Phys. Rev. Lett. **88**, 247004 (2002).

[9] N. Kokubo, K. Kadowaki, and K. Takita, Phys. Rev. Lett. **95**, 177005 (2005).

[10] N. Kokubo, T. Asada, K. Kadowaki, K. Takita, T. G. Sorop, and P. H. Kes, Phys. Rev. B **75**, 184512 (2007).

[11] U. Yaron, P. L. Gammel, D. A. Huse, R. N. Kleiman, C. S. Oglesby, E. Bucher, B. Batlogg, D. J. Bishop, K. Mortensen, and K. N. Clausen, Nature (London) **376**, 753 (1995).

[12] A. E. Koshelev and V. M. Vinokur, Phys. Rev. Lett. **73**, 3580 (1994).

[13] Y. Togawa, R. Abiru, K. Iwaya, H. Kitano, and A. Maeda, Phys. Rev. Lett. **85**, 3716 (2000).

[14] L. Balents, M. C. Marchetti, and L. Radzihovsky, Phys. Rev. B **57**, 7705 (1998).

[15] C. J. Olson, C. Reichhardt, and F. Nori, Phys. Rev. Lett. **81**, 3757 (1998).

[16] A. B. Kolton, D. Dominguez, and N. Grønbech-Jensen, Phys. Rev. Lett. **83**, 3061 (1999).

[17] A. B. Kolton, D. Dominguez, and N. Grønbech-Jensen, Phys. Rev. Lett. **86**, 4112 (2001).

[18] P. H. Kes and C. C. Tsuei, Phys. Rev. B **28**, 5126 (1983).

[19] S. Bhattacharya and M. J. Higgins, Phys. Rev. Lett. **70**, 2617 (1993).

[20] A. C. Marley, M. J. Higgins, and S. Bhattacharya, Phys. Rev. Lett. **74**, 3029 (1995).

[21] Y. Paltiel, E. Zeldov, Y. Myasoedov, M. L. Rappaport, G. Jung, S. Bhattacharya, M. J. Higgins, Z. L. Xiao, E. Y. Andrei, P. L. Gammel, and D. J. Bishop, Phys. Rev. Lett. **85**, 3712 (2000); Y. Paltiel, G. Jung, Y. Myasoedov, M. L. Rappaport, E. Zeldov, M. J. Higgins, and S. Bhattacharya, Europhys. Lett. **58**, 112 (2002).

[22] S. Okuma, J. Inoue, and N. Kokubo, *Proceedings of the 19th International Symposium on Superconductivity, Nagoya, 2006* [Physica C 463–465, 290 (2007)].

[23] S. Okuma, Y. Imamoto, and M. Morita, Phys. Rev. Lett. **86**, 3136 (2001); S. Okuma, S. Togo, and M. Morita, *ibid.* **91**, 067001 (2003); S. Okuma, M. Kobayashi, and M. Kamada, *ibid.* **94**, 047003 (2005).

[24] S. Okuma and N. Kokubo, Phys. Rev. B **61**, 671 (2000); S. Okuma and M. Kamada, *ibid.* **70**, 014509 (2004).